50-2505

Copy 85

RM A9I26

~~CONFIDENTIAL~~

53 27-77

A9I26

TECH LIBRARY KAFB, NM

0142957

6310

NACA

RESEARCH MEMORANDUM

ESTIMATION OF THE FORCES AND MOMENTS ACTING ON INCLINED BODIES OF REVOLUTION OF HIGH FINENESS RATIO

By H. Julian Allen

Ames Aeronautical Laboratory
Moffett Field, Calif.

AFMDC
TECHNICAL LIBRARY
AFL 2811

CLASSIFIED DOCUMENT

This document contains classified information affecting the National Defense of the United States within the meaning of the Espionage Act, USC 50:31 and 32. Its transmission or the revelation of its contents in any manner to an unauthorized person is prohibited by law. Information so classified may be imparted only to persons in the military and naval services of the United States, appropriate civilian officers and employees of the Federal Government who have a legitimate interest therein, and to United States citizens of known loyalty and discretion who of necessity must be informed thereof.

HOLLOMAN AFB N.M.
21 NOV 1949

NATIONAL ADVISORY COMMITTEE FOR AERONAUTICS

WASHINGTON
November 14, 1949

~~CONFIDENTIAL~~

319.98/13

50-2505

TECH LIBRARY KAFB, NM

0142957

NATIONAL ADVISORY COMMITTEE FOR AERONAUTICS

RESEARCH MEMORANDUM

ESTIMATION OF THE FORCES AND MOMENTS ACTING ON INCLINED BODIES OF REVOLUTION OF HIGH FINENESS RATIO

By H. Julian Allen

SUMMARY

This report contains a discussion of the aerodynamic forces and moments on inclined bodies of revolution. It is known that a simple potential flow solution for such bodies does not give results in good agreement with experiment. An approximate theory to allow for the effects of viscosity for such bodies is developed and applied. It is shown that a simple allowance for viscous effects yields results in reasonable agreement with experiment for bodies of high fineness ratio such as would be used on missiles and supersonic aircraft. The methods developed are applicable at both subsonic and supersonic speeds. Some discussion of the probable effects of Reynolds number and Mach number on the forces and moments on inclined bodies of revolution is included.

INTRODUCTION

Knowledge of the forces and moments on bodies of revolution has long been of interest in aeronautical engineering. The original interest pertained to the characteristics of airship hulls, and one of the first logical attempts at understanding the nature of the flow field of these relatively long closed bodies was made by Max Munk (reference 1). Munk demonstrated that on such closed bodies at a constant angle of pitch in straight flight and in a nonviscous fluid there occurred elemental forces along the hull resulting from changes in the downward momentum of the fluid. Over the forward portions of the hull shown in figure 1 the downward momentum of the fluid must increase proceeding downstream because the apparent mass of the component flow normal to the axis of revolution increases due to the enlarging cross sections of the hull. Over this portion of the hull the reaction is upwardly directed for positive angles of attack. For bodies with parallel midsection, representative of the older airships, no cross force exists over these elements of the hull since there occurs no change in momentum of the fluid as the air progresses along these sections of constant area. At the stern the contracting cross sections require a removal of momentum from the air stream and hence downwardly directed

50-2305

elemental forces exist along the hull for positive hull angles of attack. It is shown in Munk's work that for bodies of high fineness ratio the potential cross force per unit length f_p at any station along the hull is given by

$$f_p = (k_2 - k_1)\, q\, \frac{dS}{dx} \sin 2\alpha \tag{1}$$

where S is the cross-sectional area of the hull, x is the distance along the hull from the bow, α is the angle of attack,[1] and k_2 and k_1 are, respectively, the transverse and longitudinal apparent mass coefficients for the body. The variation of $k_2 - k_1$ as a function of fineness ratio is given in figure 2. This cross force at small angles of attack can be shown from the work of G. N. Ward, reference 2, to be directed midway between the normal to the axis of revolution of the hull and the normal to the direction of motion of the hull (i.e., at an angle $\alpha/2$).

It is evident that for a closed body, such as an airship hull, at a positive angle of attack the upwardly directed forces over the forward portion must be equal to the downwardly directed forces over the rear so that a pitching moment but no lift or drag results. In figures 3 and 4 are shown a comparison of calculated and experimentally determined lift and pitching moments as a function of angle of attack for the hulls of the American airship ZR-4 (U.S.S. Akron) (from reference 3) and the British airship R-32 (from reference 4). It is seen that, contrary to the prediction of theory, a significant lift force exists at angle of attack. The pitching moment is reasonably well given by the theory, although the actual magnitude of the pitching moment is less, in general, than the predicted.

Upson and Klikoff (reference 5) have compared the calculated and observed cross forces for several hull shapes, one of which is shown in figure 5. The discrepancy at the bow has been shown by Upson and Klikoff to be due to the bluffness of the body. A discrepancy also exists between calculated and experimental characteristics over the remainder of the hull, the actual cross force over the rearward surfaces always being more positive for positive pitch than the potential theory predicts. It has long been recognized that this discrepancy results from the influence of viscosity of the fluid.

In recent years the determination of the cross forces on bodies of revolution has again become of first importance to the designers of supersonic aircraft and missiles. These bodies in general differ from the usual airship hulls in two important aspects: First, the bodies are of higher fineness ratio, and, second, the bodies have a blunt stern or "base."

[1]Throughout this report cross-force characteristics are considered in terms of the angle of pitch. It is clear that for a body of revolution the arguments presented apply equally well to angles of yaw or any combinations of pitch and yaw.

It has been pointed out by Tsien (reference 6) that the older airship theories for the potential cross force are still applicable to such bodies even in supersonic flow for slender bodies at small angles of attack. For such unclosed bodies the airship theory would predict, in addition to a pitching moment, a lift and drag, but it is again to be expected that the failure to consider effects of viscosity will lead to important discrepancies between these calculated characteristics and experimental ones.

It is the purpose of this paper to present an approximate analysis of the effects of viscosity on bodies of high fineness ratio.

SYMBOLS

a speed of sound, feet per second

A characteristic reference area of body for force and moment coefficient definition, square feet

A_p plan-form area, square feet

c_{d_c} section drag coefficient of a circular cylinder per unit length in terms of its diameter

C_L body lift coefficient

C_M body moment coefficient about an arbitrary axis at distance x_m from the bow

C_D body drag coefficient

$C_{D_{\alpha=0}}$ body drag coefficient at zero angle of attack

ΔC_D increase in body drag coefficient above that at zero angle of attack

D body drag, pounds

$D_{\alpha=0}$ body drag at zero angle of attack, pounds

f cross force per unit length along the body, pounds per foot

f_p potential cross force per unit length along the body, pounds per foot

f_v viscous cross force per unit length along the body, pounds per foot

f_{v_∞} viscous cross force per unit length along the body of infinite length, pounds per foot

k_1 longitudinal apparent mass coefficient

k_2 transverse apparent mass coefficient

l actual body length, feet

l_o equivalent length of a blunt based body, feet

L lift, pounds

M moment about an arbitrary axis at distance x_m from the bow, foot-pounds

M_o free-stream Mach number

M_c cross Mach number (i.e., component Mach number of the flow normal to the axis of revolution of the body)

q free-stream dynamic pressure, pounds per square foot

r radius of the body at any station x from the bow, feet

r_o maximum body radius, feet

R_o free-stream Reynolds number

R_c cross Reynolds number (i.e., Reynolds number based on the cross velocity)

S cross-sectional area of the body at any station x from the bow, square feet

S_b cross-sectional area of the base of the body, square feet

V_o free-stream velocity, feet per second

V_c cross velocity (i.e., component of the flow velocity normal to the axis of revolution), feet per second

vol total volume of the body, cubic feet

x longitudinal distance from the bow, feet

x_p distance of the centroid of the plan-form area from the bow, feet

x_m station of the axis of moments, feet

X reference length used in definition of moment coefficient, feet

α angle of attack, degrees or radians as indicated

η ratio of the drag coefficient of a circular cylinder of finite length to that for a cylinder of infinite length

ν free-stream kinematic viscosity, feet squared per second

ρ mass density, slugs per cubic foot

THEORY

In reference 7, R. T. Jones, following earlier work of L. Prandtl in reference 8, considered the effects of viscosity on the flow over infinitely long yawed cylinders and demonstrated that in the case of a laminar flow the viscous effects may be considered by treating the flow across the cylinder axis independently of the flow along the cylinder. For circular cylinders of infinite length the viscous force along the cylinder is simply that due to surface shear. The component flow across the cylinder, however, introduces large cross forces due to separation of the flow. Jones has shown that the cross force on a yawed cylinder is accurately determined by considering the cross component of drag as may be seen in figure 6 taken from reference 7. Although the demonstration of reference 7 applies to laminar flows, it will be assumed to be applicable to turbulent flows as well.

Consider, now, a body of revolution of high fineness ratio. It is again to be expected that the cross-force characteristics could be approximately predicted by treating each circular cross section as an element of an infinitely long circular cylinder of the same cross-sectional area. With this assumption the local cross force per unit length due to viscosity f_{v_∞} would be given by

$$f_{v_\infty} = 2rc_{d_c} \frac{\rho V_c^{\,2}}{2} \tag{2}$$

where r is the body radius at any station x from the bow, V_c is the cross velocity, ρ is the mass density, and c_{d_c} is the drag coefficient of a circular cylinder at the Reynolds number

$$R_c = \frac{2rV_c}{\nu} \tag{3}$$

and the Mach number

$$M_c = \frac{V_c}{a} \tag{4}$$

where, in addition, ν is the kinematic viscosity, and a is the speed

of sound in the undisturbed stream.

Since the cross velocity

$$V_c = V_o \sin \alpha \tag{5}$$

it follows that the viscous cross force becomes

$$f_{v_\infty} = 2rc_{d_c}\, q \sin^2 \alpha \tag{6}$$

where q is the dynamic pressure. The cross drag coefficient c_{d_c} is that of a circular cylinder at the cross Reynolds number

$$R_c = \frac{2rV_o}{\nu} \sin \alpha = R_o \sin \alpha \tag{7}$$

and the cross Mach number

$$M_c = M_o \sin \alpha \tag{8}$$

where M_o is the Mach number of the free stream.

It is known (see appendix) that the drag coefficient of a circular cylinder of finite length is less than that for a cylinder of infinite length. A similar characteristic is to be expected as regards the viscous cross force for a body of finite length in oblique flow so that the viscous cross force will be less than that given by equation (6). It is almost certain that the largest portion of the drag reduction due to finite length occurs at the ends of the cylinder. It will be assumed, however, that the reduction in drag for fineness ratio is the same for each element of a body of finite length so that in that case the viscous cross force becomes

$$f_v = 2\eta rc_{d_c}\, q \sin^2 \alpha \tag{9}$$

where η is the ratio of cross drag coefficient for the body of finite fineness ratio to that for a body of infinite fineness ratio.

The integrated viscous cross force is then

$$2\eta q \sin^2 \alpha \int_0^l rc_{d_c}\, dx$$

where l is the body length.

In determination of the lift and drag characteristics at angle of attack, it should be noted that there also exists a viscous axial force

which is approximately the total drag at zero angle reduced by the reduction in axial dynamic pressure. The viscous axial force is then

$$C_{D_{\alpha=0}}\ q\ A\ \cos^2\alpha \tag{10}$$

where $C_{D_{\alpha=0}}$ is the drag coefficient at zero angle and A is the area upon which this coefficient is based.

It is now assumed that the potential solution of Munk and the viscous solution may be combined to determine the cross-force distribution along the body and the integrated forces and moment on the body. The potential cross force per unit length acts at an angle $\alpha/2$ from the normal to the free-stream direction, while the viscous force acts normal to the axis of revolution of the body so that the distribution of cross force in terms of the dynamic pressure is given, from equations (1) and (9), by

$$\frac{f}{q} = \frac{f_p}{q}\cos\frac{\alpha}{2} + \frac{f_v}{q}$$

or

$$\frac{f}{q} = (k_2-k_1)\frac{dS}{dx}\sin 2\alpha\cos\frac{\alpha}{2} + 2\eta r c_{d_c}\sin^2\alpha \tag{11}$$

The lift coefficient in terms of the reference area A is given by

$$C_L = \frac{L}{qA}$$

where L is the total lift. Consideration of the potential cross force, the viscous cross force, and the viscous axial force then yields

$$C_L = \frac{(k_2-k_1)\sin 2\alpha\cos\frac{\alpha}{2}}{A}\int_0^l \frac{dS}{dx}\,dx + \frac{2\eta\sin^2\alpha\cos\alpha}{A}\int_0^l r c_{d_c}\,dx - C_{D_{\alpha=0}}\cos^2\alpha\sin\alpha \tag{12}$$

The drag coefficient is obtained from the cross and axial forces as

$$C_D = \frac{D}{qA}$$

where D is the total drag, or

$$C_D = \frac{(k_2-k_1)\ \sin 2\alpha\ \sin\frac{\alpha}{2}}{A}\int_0^l \frac{dS}{dx}\,dx + \frac{2\eta\ \sin^3\alpha}{A}\int_0^l rc_{d_c}\,dx + C_{D_{\alpha=0}}\cos^3\alpha \tag{13}$$

The moment coefficient about a given station x_m is dependent solely upon the cross-force distribution and is given by

$$C_M = \frac{M}{qAX}$$

$$C_M = \frac{(k_2-k_1)\ \sin 2\alpha\ \cos\frac{\alpha}{2}}{AX}\int_0^l \frac{dS}{dx}(x_m-x)\,dx + \frac{2\eta\ \sin^2\alpha}{AX}\int_0^l rc_{d_c}(x_m-x)\,dx \tag{14}$$

where X is a characteristic length for the evaluation of moment coefficient.

The method of the present report is clearly too approximate to justify the implied accuracy of the preceding equations. It is considered that, in general, the following simplifications are warranted:

1. Cosines of angles should be replaced by unity and sines of angles by the angles.

2. The factor k_2-k_1 should be replaced by unity.

3. The viscous axial force (third) term of equation (12) may be neglected, while the corresponding term in equation (13) may be replaced by $C_{D_{\alpha=0}}$.

Moreover the potential term integrals may be evaluated as

$$\int_0^l \frac{dS}{dx}\,dx = S_b$$

and

$$\int_0^l \frac{dS}{dx}(x_m-x)\,dx = \text{vol} - S_b(l-x_m)$$

where S_b is the area of the body base and vol is the body volume.

The viscous cross-force term integrals may also be evaluated as

$$\int_0^l r dx = \frac{1}{2} A_p$$

and

$$\int_0^l r(x_m - x) dx = \frac{1}{2} A_p (x_m - x_p)$$

where A_p is the plan-form area and x_p is the distance to its centroid from the bow.

With the indicated changes equations (11) to (14) become, respectively (with α in radians),

$$\frac{f}{q} = 2\left(\frac{dS}{dx}\right)\alpha + 2\eta c_{d_c} r \alpha^2 \tag{11a}$$

$$C_L = 2\left(\frac{S_b}{A}\right)\alpha + \eta c_{d_c}\left(\frac{A_p}{A}\right)\alpha^2 \tag{12a}$$

$$\Delta C_D = C_D - C_{D_{\alpha=0}} = \left(\frac{S_b}{A}\right)\alpha^2 + \eta c_{d_c}\left(\frac{A_p}{A}\right)\alpha^3 \tag{13a}$$

and

$$C_M = 2\left[\frac{\text{vol} - S_b(l - x_m)}{AX}\right]\alpha + \eta c_{d_c}\left(\frac{A_p}{A}\right)\left(\frac{x_m - x_p}{X}\right)\alpha^2 \tag{14a}$$

To determine the force and moment characteristics it is necessary to evaluate the coefficients η and c_{d_c}. In the appendix, available data and some discussion of the coefficients are given.

Comparison of Theory and Experiment

Tests were recently completed at the Ames Aeronautical Laboratory of the high-fineness-ratio body shown in figure 7. The tests were conducted in the subsonic speed range in the 12-foot pressure tunnel (reference 9), and in the supersonic speed range in the 6- by 6-foot wind tunnel (as yet unreported). The test results afforded a good opportunity to compare the theory of this report with experiment.

In none of the tests did the cross Mach number (given by equation (8)) exceed 0.3 so that, as may be seen from the appendix, no sensible compressibility effect exists, while the cross Reynolds number remained in the range for which c_{d_c} is constant and equal to 1.2. The coefficient η was assumed to be dictated by the actual fineness ratio

$$\frac{l}{2r_o} = \frac{3.912}{0.396} \cong 9.9$$

for which

$$\eta = 0.68$$

With these values and the geometric parameters obtained from the shape equation (see fig. 7) the equations for lift coefficient, drag-coefficient increment, and moment coefficient may be determined from equations (12a) to (14a) as (with α in degrees)

$$C_L = \frac{L}{qA} = 0.019\ \alpha + 0.0025\ \alpha^2$$

$$\Delta C_D = \frac{D-D_{\alpha=0}}{qA} = 0.00017\ \alpha^2 + 0.000043\ \alpha^3$$

$$C_M = \frac{M}{qAl} = 0.018\ \alpha + 0.00035\ \alpha^2$$

where A and l are the maximum cross-sectional area and the actual body length, respectively, and the pitching moment is about a point

$$x_m = 0.704\ l$$

which is the point about which the moments were considered in the experimental investigation of reference 9. The calculated characteristics of lift, drag increment, and pitching moment are compared with the experimental values in figure 8. It is seen that the theory of this report well predicts the lift and drag variation with angle of attack. The magnitude of the experimental values of the pitching moment are lower, however, than the theory of this report would predict.

DISCUSSION AND CONCLUDING REMARKS

It is evident from equations (12a) and (14a) that the variation of lift and pitching moment of a body of revolution with angle of attack must, in the general case, be nonlinear since the potential cross forces due to the change of momentum of the fluid varies as the first power in α while the viscous cross force varies as the second power of the angle of attack. This is a particularly important aspect in the design of missiles since the guidance and control problem will be affected if nonlinear characteristics exist. It is of interest to note from equation (14a) that the pitching-moment variation about the center of gravity for constant cross-force drag coefficient will be linear if the center of gravity is located at the centroid of the plan-form area.

From the theory of this report, it appears possible to make the pitching-moment variation about the center of gravity of the body zero in one special case. This is the case of the body for which

$$\frac{dS}{dx} = 2\pi r \frac{dr}{dx} \approx r$$

that is, a conical body

$$r \approx x$$

if the center of gravity is at the centroid of the cross area.

Several other important expectations may be implied from the theory of this report: First, since the cross Reynolds number, which determines the cross drag coefficient, varies with angle of attack, it is possible for the cross drag coefficient to rather abruptly change (when R_c varies with angle from 2×10^5 to 5×10^5) with angle of attack which might lead to rather erratic variations of the forces and moments with angle of attack. However, it is to be expected that the three-dimensional effects previously mentioned will reduce the indicated abrupt behavior. It is also to be noted that wind-tunnel tests at lower scales would not necessarily show these peculiarities. Second, for bodies moving at high speeds the cross Mach number will increase from subsonic to supersonic values as the angle of attack is increased and the cross drag coefficient may vary in an erratic manner. This variation may again lead to corresponding variation in the forces and moment with angle of attack. Thus it is clear that model tests of high-speed missiles should be performed over the whole speed range expected for the configuration if the model tests are to be indicative of the true behavior. However, the fact that cross Reynolds number as indicated in the appendix is not important at Mach numbers above 0.5 indicates that wind-tunnel tests on small-scale models at high supersonic speeds should accurately predict the behavior of the full-scale configurations at and above the angle of attack for which the cross Mach number exceeds 0.5.

Ames Aeronautical Laboratory,
National Advisory Committee for Aeronautics,
Moffett Field, Calif.

APPENDIX

The section drag coefficients of circular cylinders have been determined for a wide range of Mach and Reynolds numbers by a number of experimenters. A fairly comprehensive discussion of the drag phenomena of circular cylinders is given in reference 10.

In figure 9 is shown the drag coefficient c_{d_c} as a function of Mach number for circular cylinders of different sizes (corresponding to different Reynolds numbers). These values were obtained by W. F. Lindsey (reference 11), John Stack (reference 12), T. E. Stanton (reference 13), and A. Busemann (reference 14), as well as from some unpublished tests performed in the Ames 1- by 3-1/2-foot high-speed wind tunnel.[2] It will be seen that Reynolds number appears of significance only at low Mach numbers, so that for values of cross Mach number higher than 0.5 the curve of figure 9 may be expected to apply for all Reynolds numbers higher than about 10^2. The variation of the drag coefficient c_{d_c} with Reynolds number is shown in figure 10 along with some of the high subsonic drag characteristics shown in figure 9 and with the curves of E. F. Relf (reference 15) and C. Wieselsberger (reference 16). Between figures 9 and 10, the drag characteristics of circular cylinders as a function of Reynolds and Mach number are fairly completely established.

The position is not so fortunate with regard to η, the ratio of the drag coefficient of circular cylinder of finite length to that of a circular cylinder of infinite length, in that this ratio, to the author's knowledge, has only been determined at one Reynolds number (88,000) and at a negligibly low Mach number (reference 10). These results are given in figure 11 and correspond to the Reynolds number range for which 1.2 is the drag coefficient of the cylinder of infinite length.

To obtain a rough estimate of the value of η at other Reynolds and Mach numbers, the following conjecture is given. The end-relieving effect for a cylinder of finite length must be primarily conveyed to other sections through the low-velocity regions in the wake. Evidently the ratio of the spanwise length of the wake to the wake thickness would be the ratio which should determine η. The spanwise length of the wake will be approximately the length of the cylinder, while the wake thickness will be nearly proportional to the product of the cylinder diameter and the drag coefficient. It appears, then, that the value of η at Reynolds and Mach numbers for which c_{d_c} is not 1.2 would be the value of η (from fig. 11) for an effective cylinder length-to-diameter ratio equal to the product of the actual length-to-diameter ratio and the ratio of the drag coefficient 1.2 to the section drag coefficient at the Reynolds and Mach number in the case considered.

---

[2] The 1- by 3-1/2-foot tunnel values (mainly useful in defining the trend at high subsonic values) were obtained using a rake of unshielded total-head tube and indicated drag coefficients about 15 percent higher than those obtained by others. It is believed that this effect was due to excessive angularity of the flow at the rake which would indicate incorrectly high values. The values have been proportionately reduced to agree with Lindsey's values and this proportionate reduction has been applied at all other Mach numbers.

It should not be considered that, because the section drag coefficients have been given for supersonic Mach numbers, the equations developed in the report are applicable at supersonic cross Mach numbers. The potential solution of Munk is derived on the assumption of an incompressible flow. This momentum solution, however, should be reasonably accurate up to cross Mach numbers of the order of 0.4. Lighthill (reference 17) has treated the problem of the inviscid cross force on bodies for the case in which the cross Mach number is not necessarily small. The solution obtained is given in increasing powers of the angle of attack. Lighthill's solution, although numerically complex, may serve to replace the inviscid portions of the equations of this report.

REFERENCES

1. Munk, Max M.: The Aerodynamic Forces on Airship Hulls. NACA Rep. 184, 1924.

2. Ward, G. N.: Supersonic Flow Past Slender Pointed Bodies. Quarterly Journ. of Mechanics and Applied Mathematics, vol. 2 Part I, Mar. 1949, pp. 75-97.

3. Freeman, Hugh B.: Force Measurements on a 1/40-Scale Model of the U. S. Airship "Akron." NACA Rep. 432, 1932.

4. Jones, R., Williams, D. H., and Bell, A. H.: Experiments on Model of a Rigid Airship of New Design. R. & M. No. 802, June 1922.

5. Upson, Ralph H., and Klikoff, W. A.: Application of Practical Hydrodynamics to Airship Design. NACA Rep. 405, 1931.

6. Tsien, Hsue-Shen: Supersonic Flow over an Inclined Body of Revolution. Jour. Aero. Sci. vol. 5, no. 12, Oct. 1938, pp. 480-483.

7. Jones, Robert T.: Effects of Sweepback on Boundary Layer and Separation. NACA Rep. 884, 1947.

8. Prandtl, L.: On Boundary Layers in Three-Dimensional Flow. M.A.P. Volkenrode Reports and Translations No. 64, May 1, 1946. (Available from Navy as trans. CGD-681.)

9. Jones, J. Lloyd, and Demele, Fred A.: Aerodynamic Study of a Wing-Fuselage Combination Employing a Wing Swept Back 63°.- Characteristics Throughout the Subsonic Speed Range with the Wing Cambered and Twisted for a Uniform Load at a Lift Coefficient of 0.25. NACA RM A9D25, 1949.

10. Goldstein, S.: Modern Developments in Fluid Dynamics. Oxford, The Clarendon Press, v. 2. Sec. 195, 1938, pp. 439-440.

11. Lindsey, W. F.: Drag of Cylinders of Simple Shapes. NACA Rep. 619, 1938.

12. Stack, John: Compressibility Effects in Aeronautical Engineering. NACA ACR, 1941.

13. Stanton, T. E.: On the Effect of Air Compression on Drag and Pressure Distribution in Cylinders of Infinite Aspect Ratio. R. & M. No. 1210, Nov. 1928.

14. von Kármán, Th.: The Problem of Resistance in Compressible Fluids. Rome, Réale Accademia D'Italia, 1936 – XIV.

15. Relf, E. F.: Discussion of the Results of Measurements of the Resistance of Wires, with Some Additional Tests on the Resistance of Wires of Small Diameter. R. & M. No. 102, British A.C.A., 1914.

16. Wieselsberger, C.: New Data on the Laws of Fluid Resistance. NACA TN 84, 1922.

17. Lighthill, M. J.: Supersonic Flow Past Slender Pointed Bodies of Revolution at Yaw. Quarterly Jour. Mech. and Applied Math., vol. I, Part 1, March 1948, pp. 76 and 89.

CONFIDENTIAL

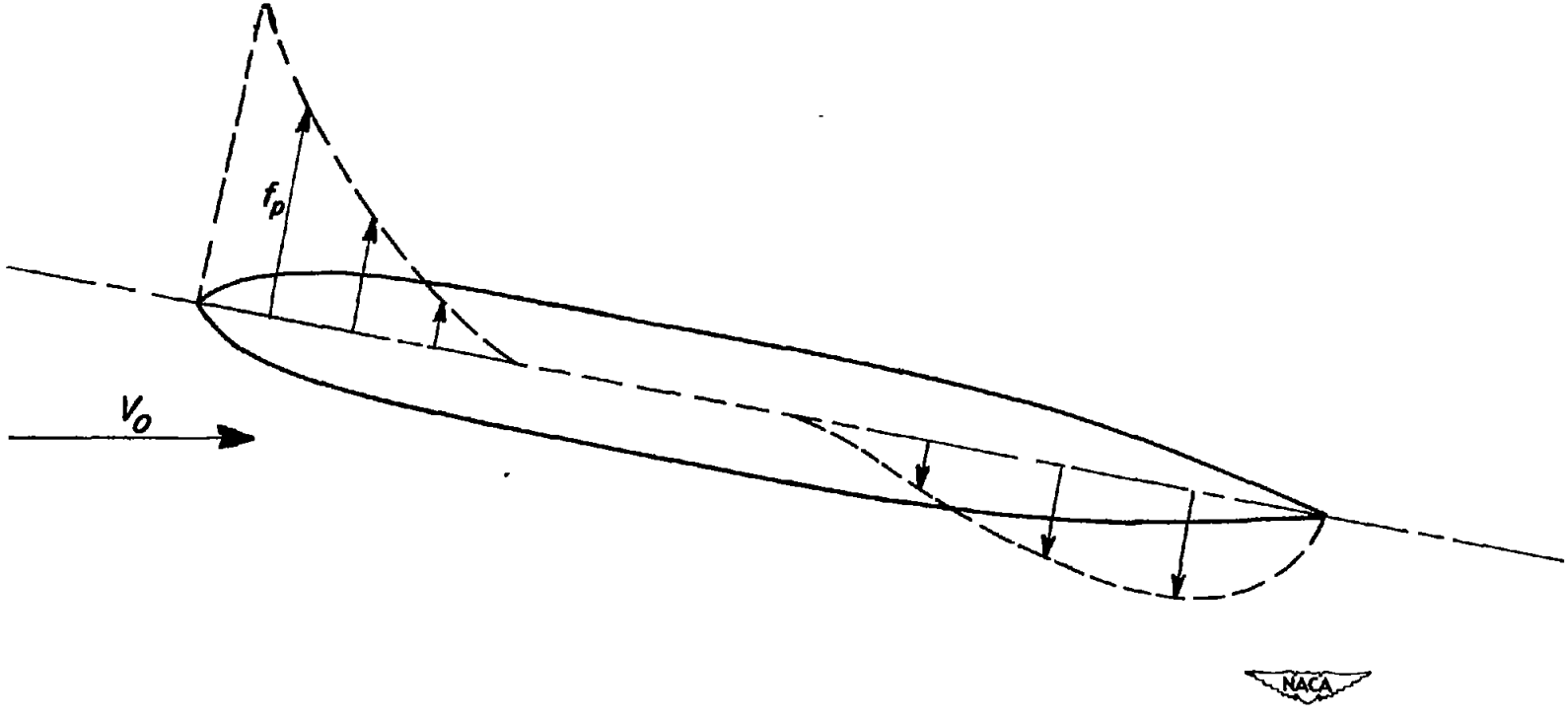

Figure 1.- Schematic diagram of the potential cross-force distribution on a body of revolution.

CONFIDENTIAL

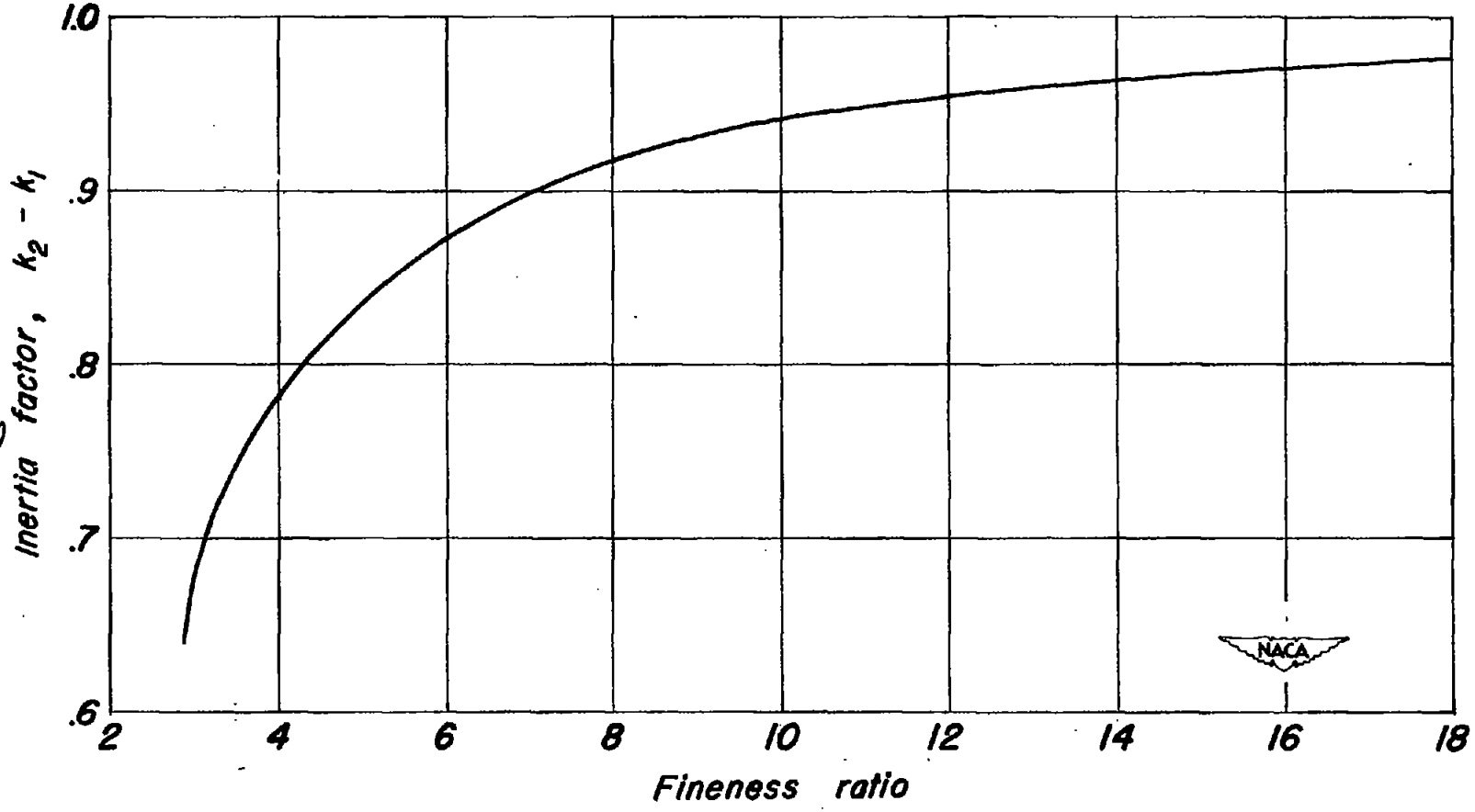

Figure 2.- Inertia factors for bodies of revolution.

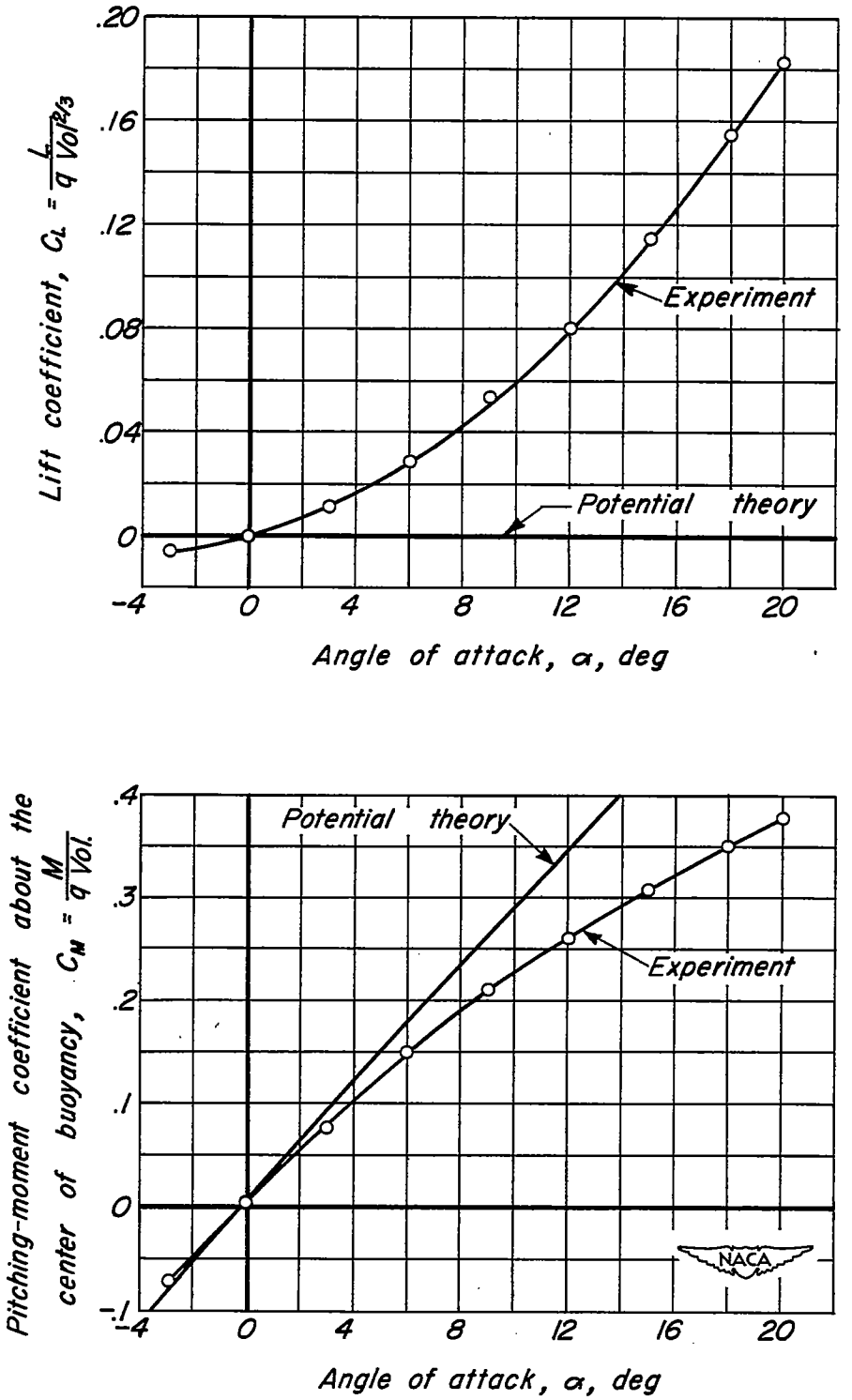

Figure 3.- Lift and pitching-moment characteristics of a hull model of the U.S.S. Akron.

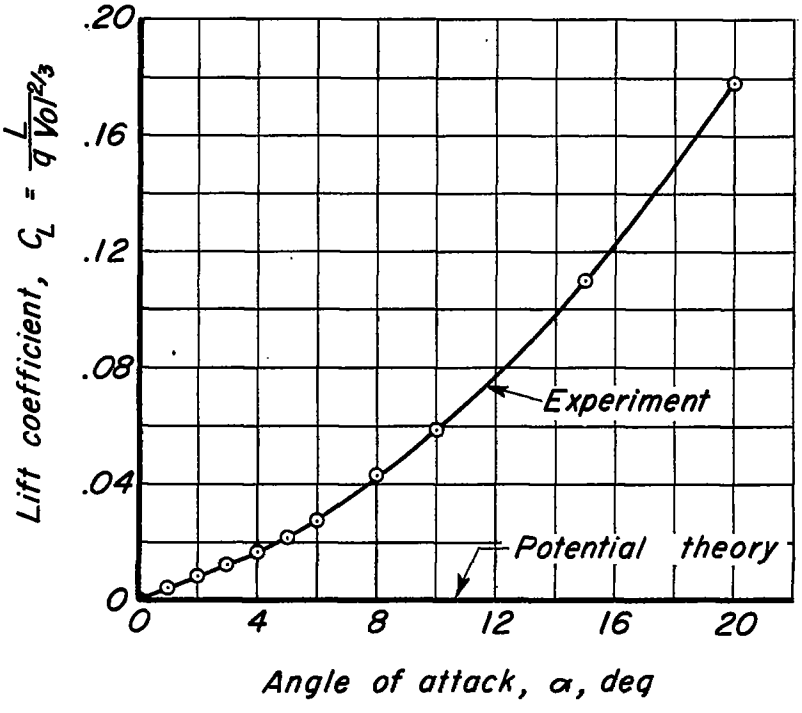

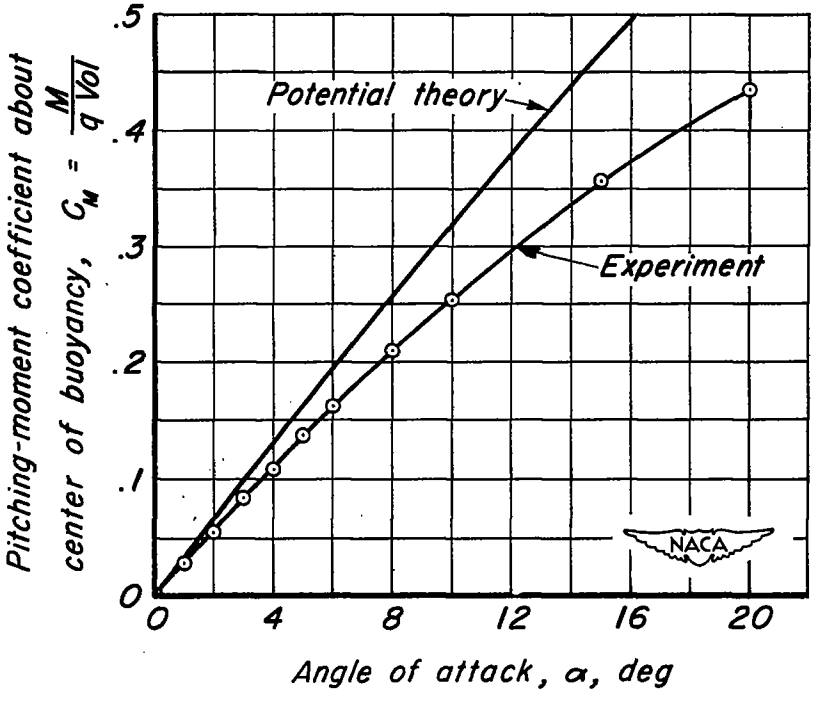

Figure 4.- Lift and pitching-moment characteristics of a hull model of the R-32.

CONFIDENTIAL

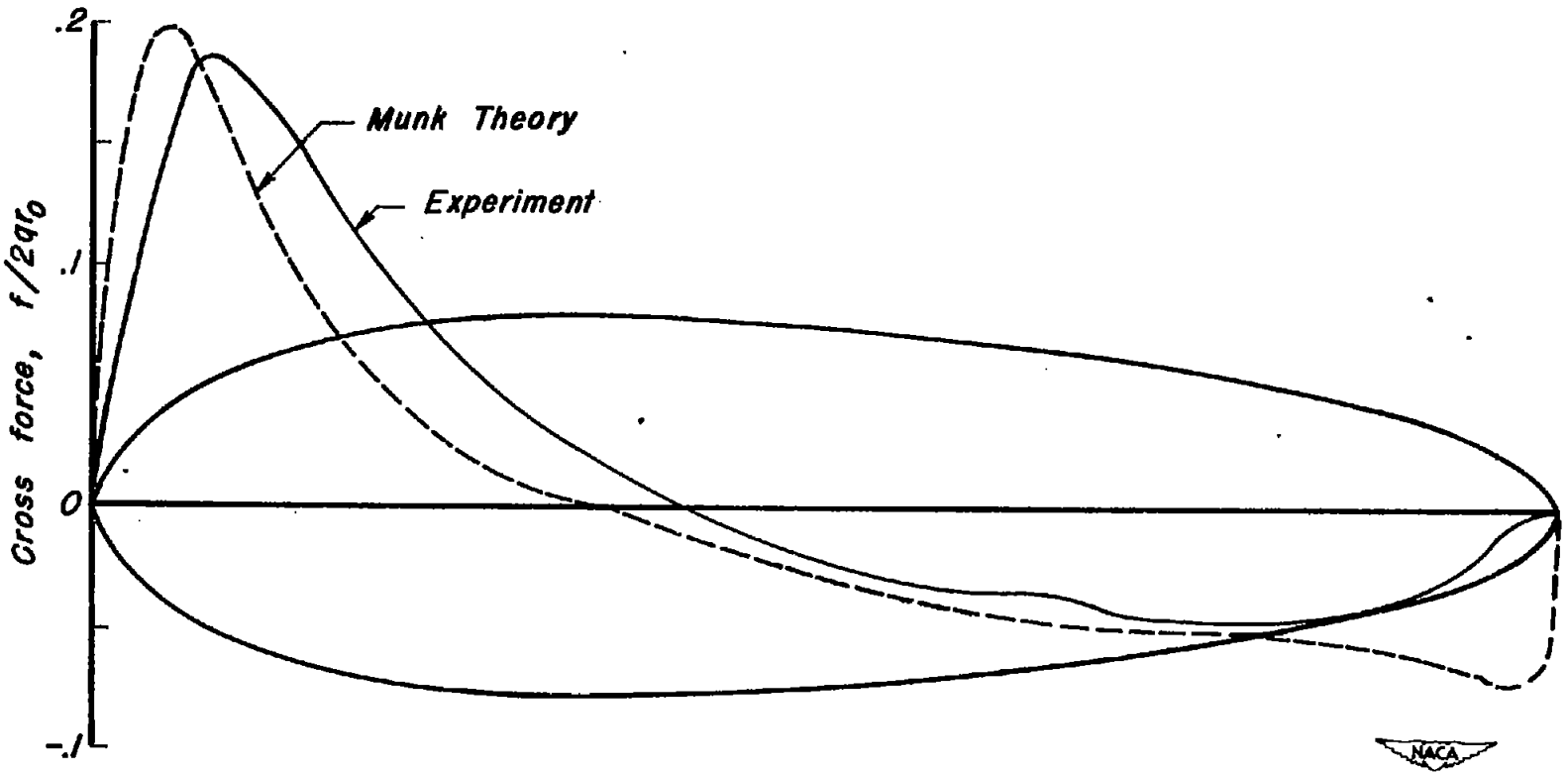

Figure 5.- Calculated and experimental cross-force distribution on a model of the semi-rigid airship, RS-1.

CONFIDENTIAL

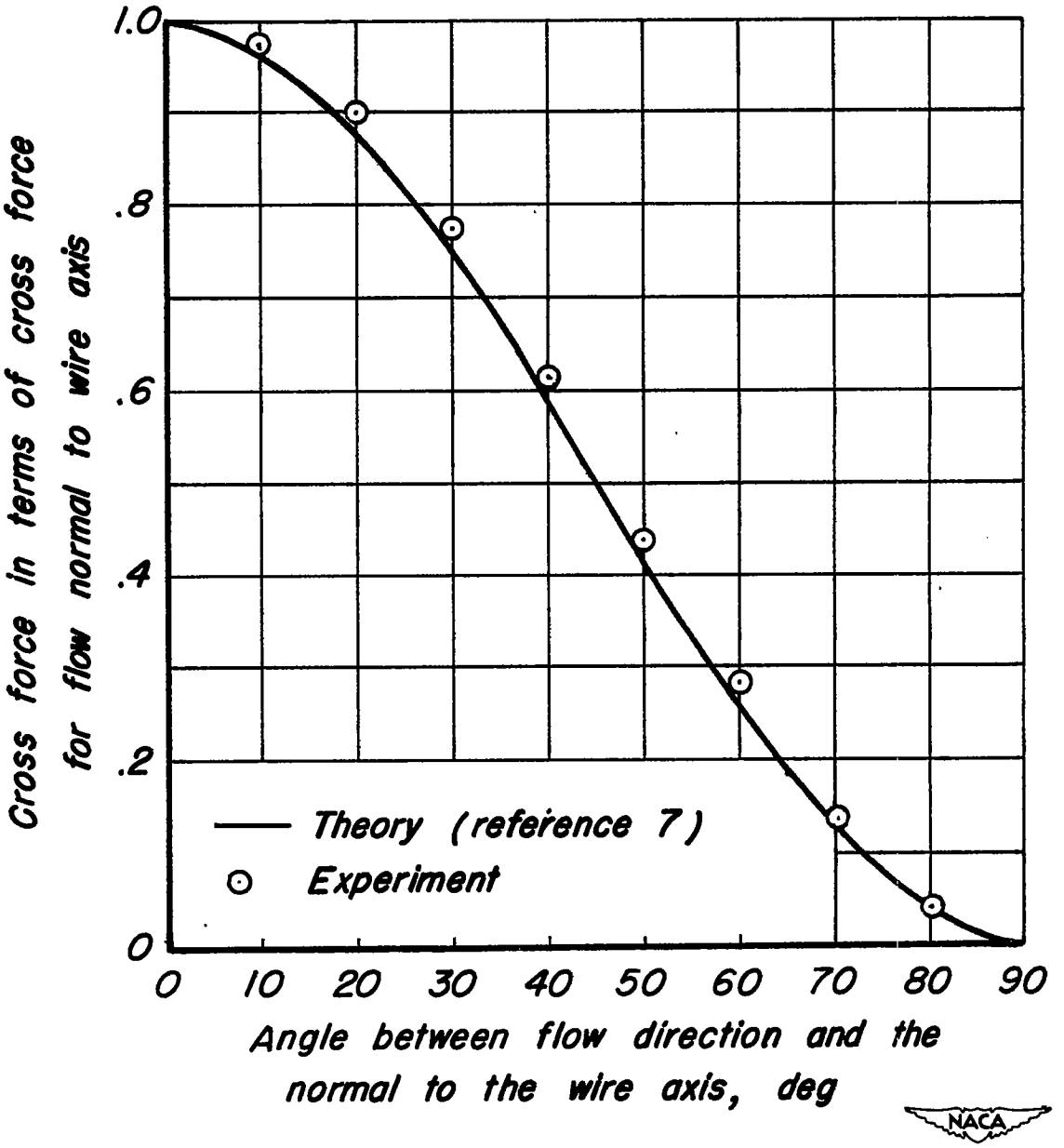

Figure 6.- Variation of cross force on an oblique wire of circular cross-section.

CONFIDENTIAL

Shape equation:

$$\frac{r}{r_0} = \left[1 - \left(1 - \frac{2x}{l_0}\right)^2\right]^{3/4}$$

Dimensions in feet

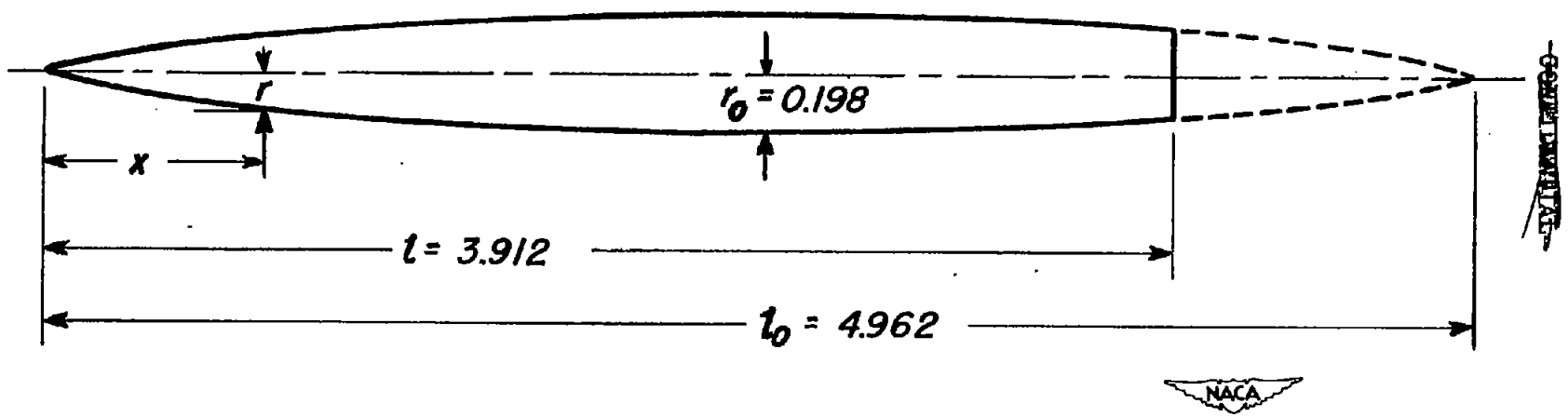

Figure 7.- Body of revolution employed for the example of this report.

CONFIDENTIAL

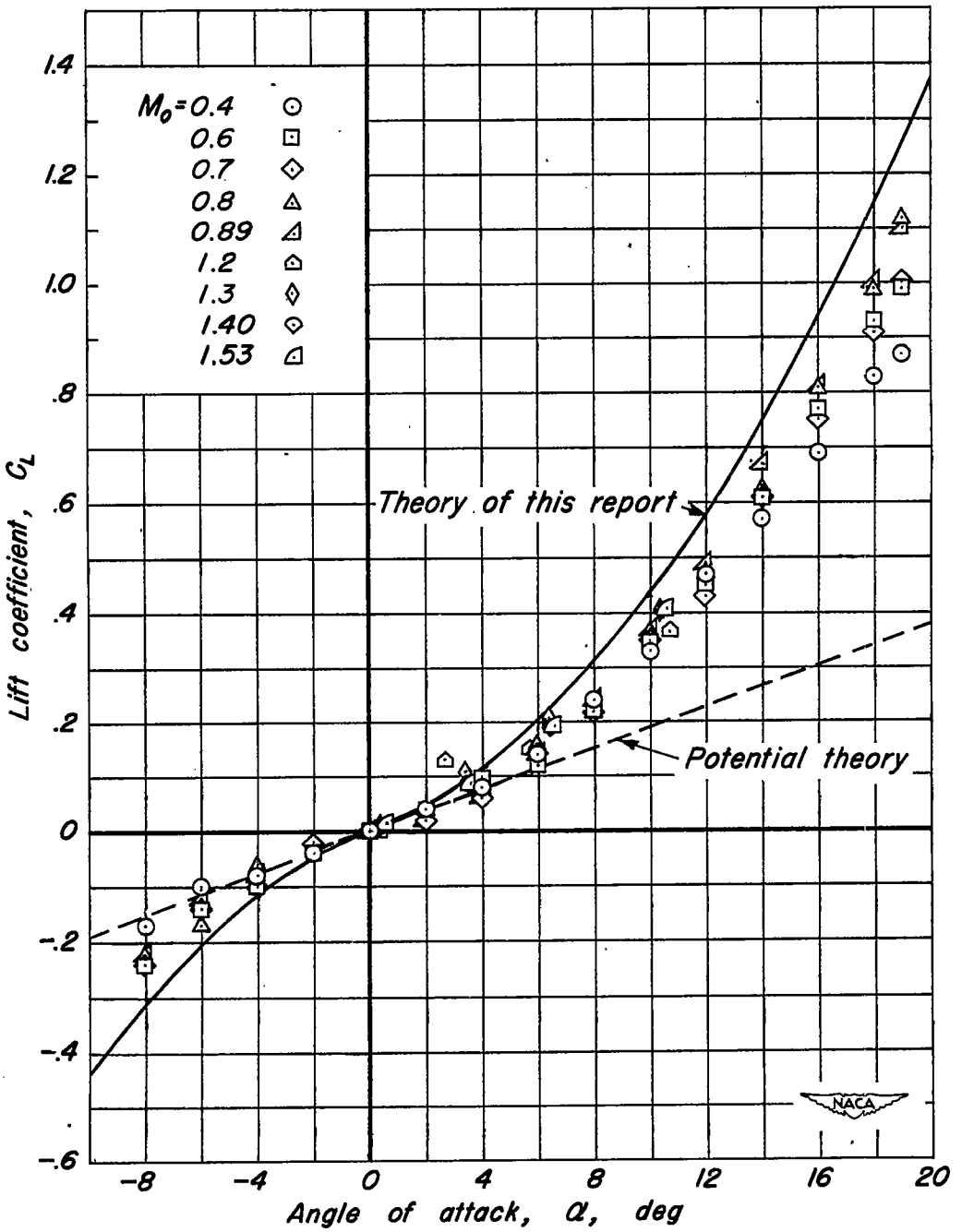

(a) Lift characteristics.

Figure 8.- Calculated and experimental aerodynamic characteristics for the example body of revolution.

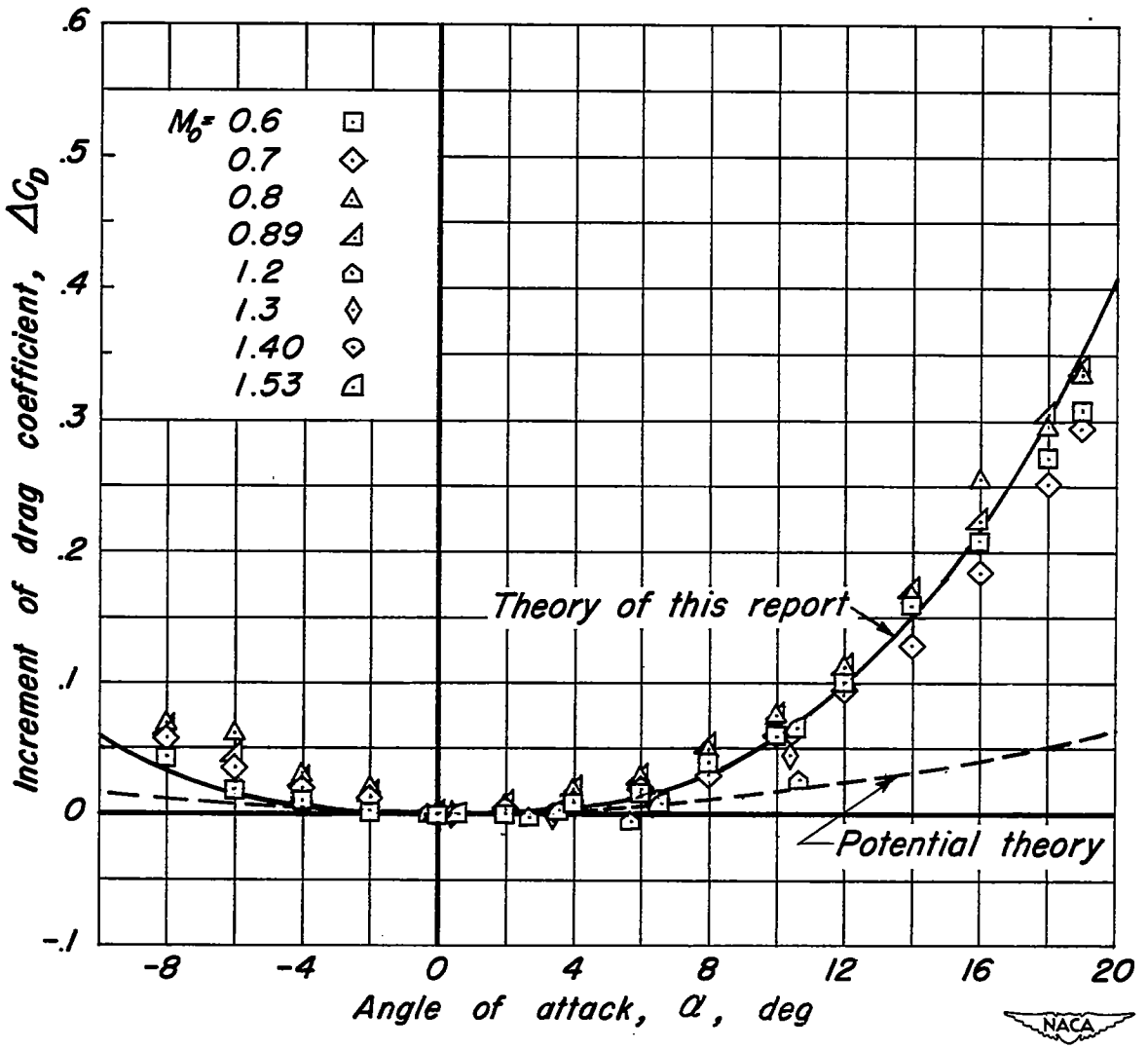

(b) Drag characteristics.

Figure 8.- Continued.

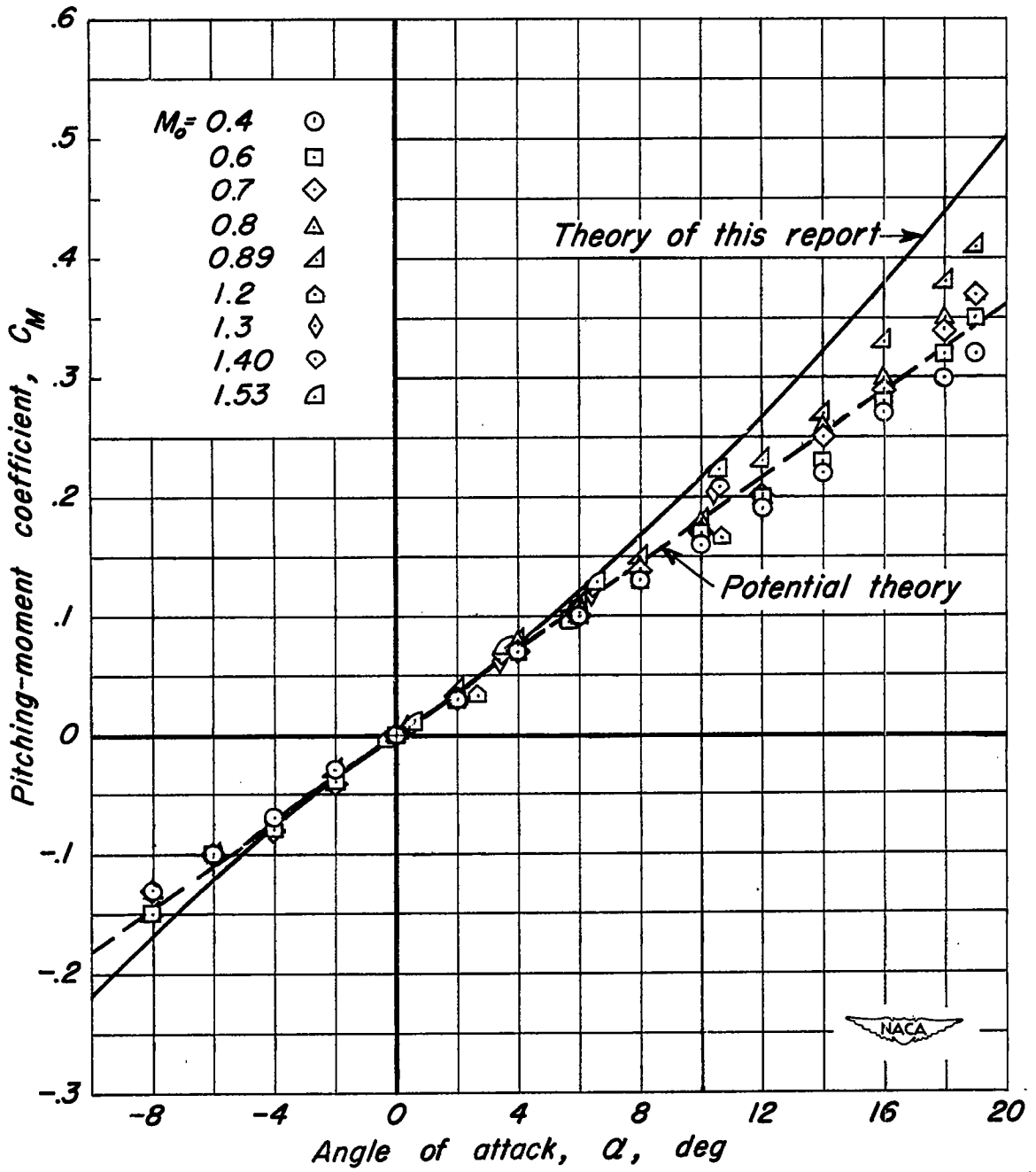

(c) Pitching-moment characteristics.

Figure 8.- Concluded.

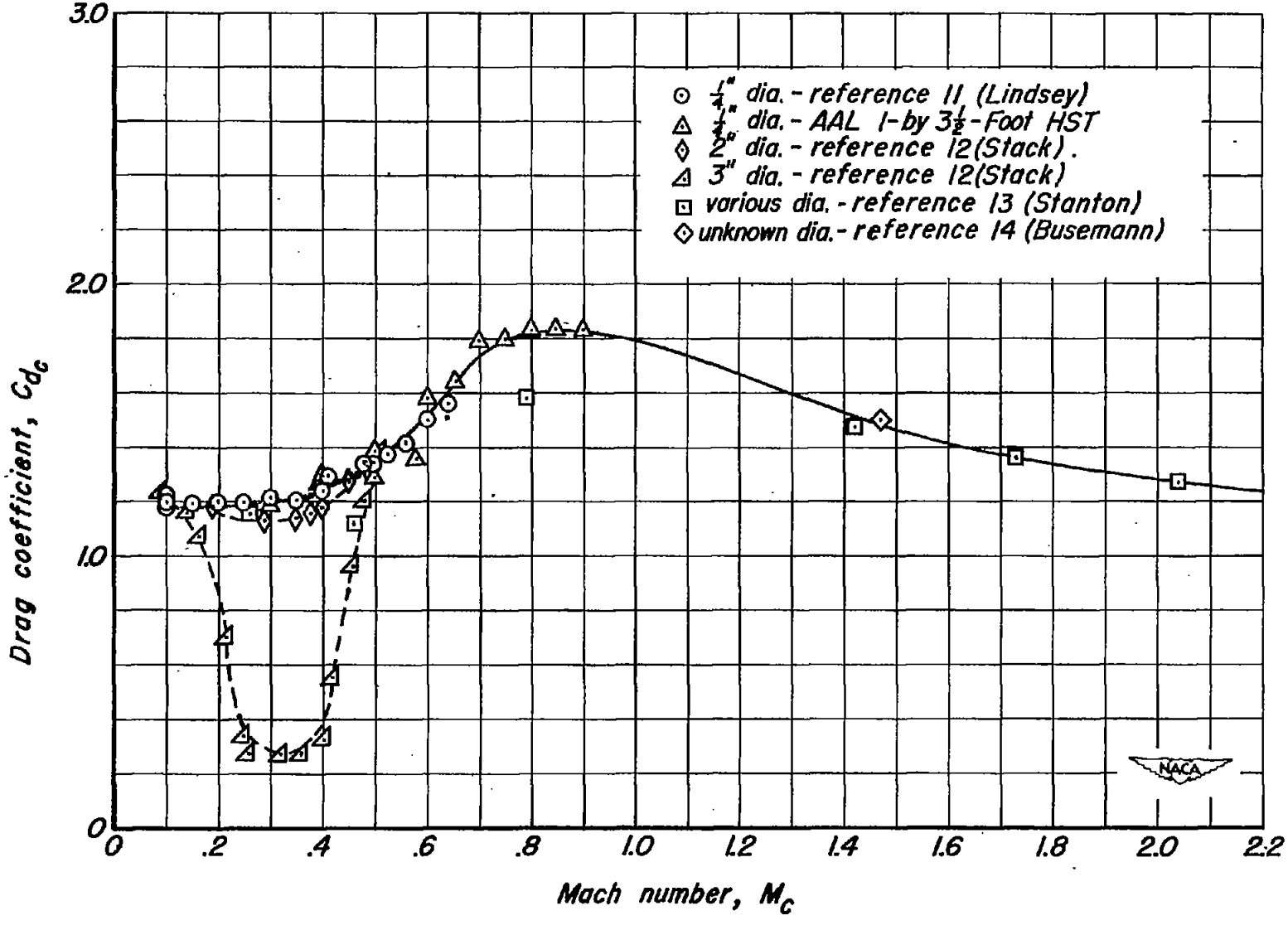

Figure 9. — Drag coefficients of circular cylinders of various sizes as a function of Mach number.

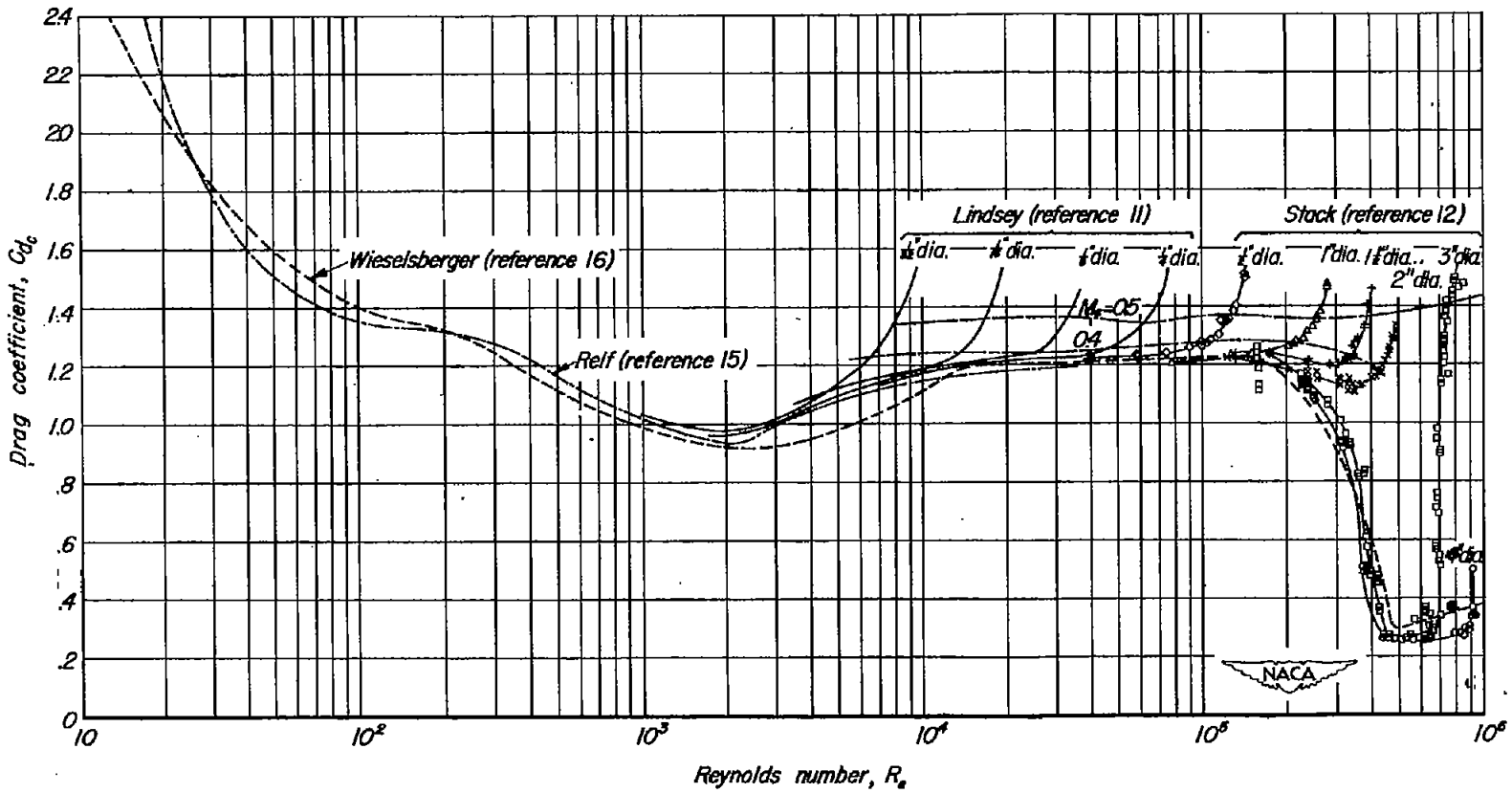

Figure 10.- Circular cylinder drag coefficient as a function of Reynolds number.

CONFIDENTIAL

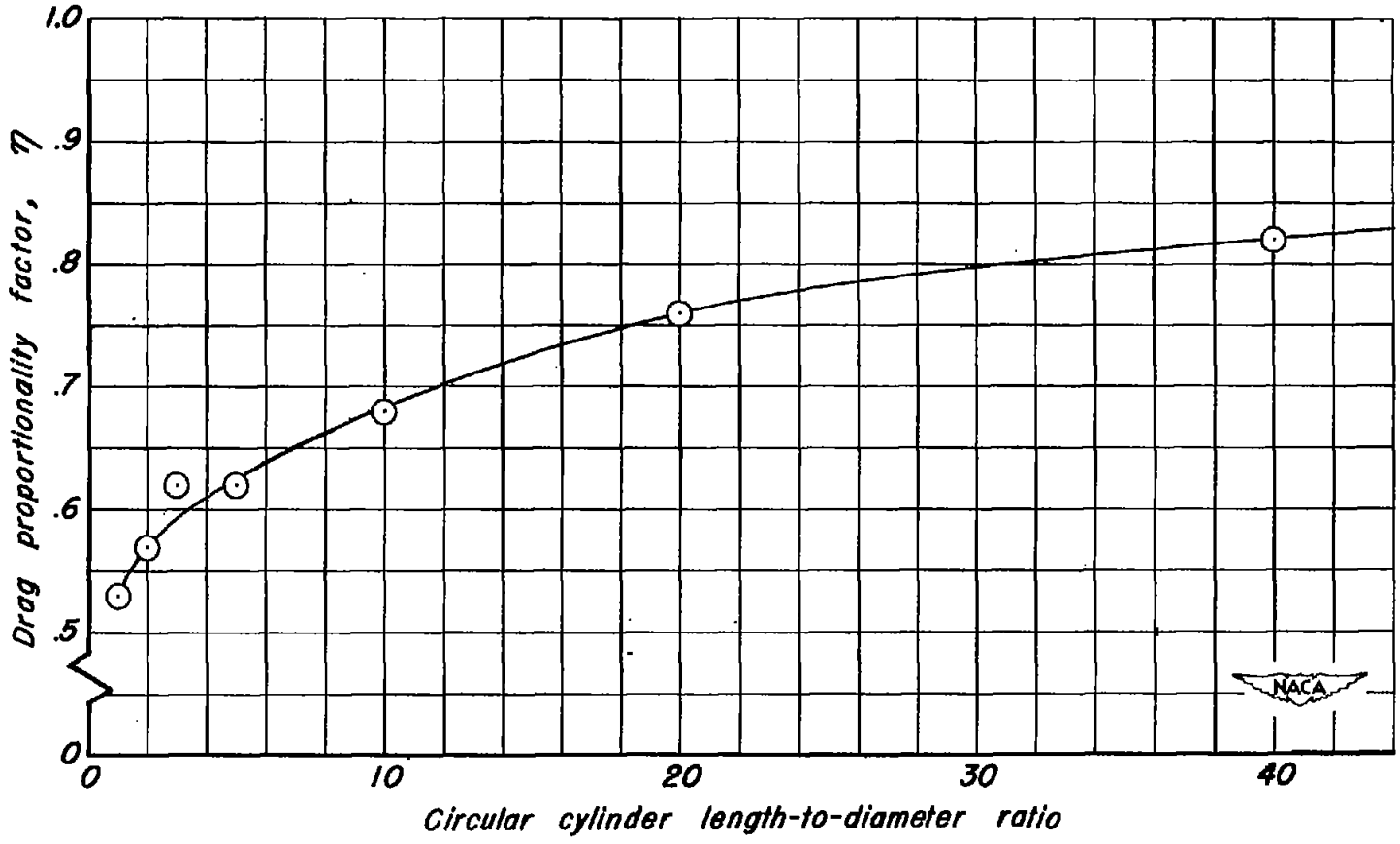

Figure 11.- Ratio of the drag coefficient of a circular cylinder of finite length to that of a cylinder of infinite length, η, as a function of the length-to-diameter ratio. (R_c=88,000)

CONFIDENTIAL

NACA-Langley - 11-14-49 - 400